Inorg. Chem. **2007**, *46*, 9126–9138

Polypyridyl Ruthenium(II) Complexes with Tetrazolate-Based Chelating Ligands. Synthesis, Reactivity, and Electrochemical and Photophysical Properties

Stefano Stagni,*,† Enrico Orselli,‡,§ Antonio Palazzi,*,† Luisa De Cola,*,‡,§ Stefano Zacchini,† Cristina Femoni,† Massimo Marcaccio,|| Francesco Paolucci,|| and Simone Zanarini||

Dipartimento di Chimica Fisica ed Inorganica, Università di Bologna, viale Risorgimento 4, I-40136 Bologna, Italy, Physikalisches Institut, Westfälische Wilhelms-Universität Münster, Mendelstrasse 7, 48149 Münster, Germany, Center for Nanotechnology (CeNTech), Heisenbergstrasse 11, 48149 Münster, Germany, and Dipartimento di Chimica "G. Ciamician", Università di Bologna, via Selmi 2, I-40126 Bologna, Italy

Received June 13, 2007

In this contribution, we report the synthesis, the chemical and photophysical characterization, and the study of the reactivity toward electrophiles of two mononuclear complexes of the type $[Ru(bpy)_2L]^+$ (bpy is 2,2′-bipyridyl), in which L is represented by the deprotonated form of 2-(*1,H*-tetrazol-5-yl)pyridine (**L1**) or 2-(*1,H*-tetrazol-5-yl)pyrazine (**L2**). The ^1H and ^{13}C NMR experiments that were performed on complexes Ru**L1** and Ru**L2** allowed us to establish that the tetrazolate moiety is bonded to the metal center via the N-1 nitrogen, while the coplanar arrangement adopted by the coordinated ligand upon coordination and the consequent interannular conjugation effect accounts for the unexpectedly low field resonance of the tetrazole carbon. The ^{13}C NMR spectroscopy is also of fundamental importance to determine the chemo- and regioselectivity of the addition of a methyl group to Ru**L1** and Ru**L2**, which takes place at the N-3 nitrogen of the five-membered ring. All these features were confirmed by the X-ray diffraction structures of Ru**L1** and of the methylated compounds Ru**L1**Me and Ru**L2**Me. Relative to these latter complexes, the presence of a methyl moiety does not cause any distortion from coplanarity of the coordinated tetrazolates. The redox properties of the complexes were investigated by cyclic voltammetry and indicated a quite different behavior between the pyrazinyl–tetrazolate and the pyridyl–tetrazolate complexes as the consequence of the higher electron-withdrawing character of the pyrazine ring. The study of the photophysical properties of the complexes also shows a significant diversity between the luminescent Ru**L1** and the rather poorly emissive Ru**L2**. Interestingly, the methylated compounds Ru**L1**Me and Ru**L2**Me display radiative excited-state decays with longer lifetimes than their precursors; this feature indicates that methylation is a useful reaction for the tuning of the light emission performances of similar tetrazolate complexes. The synthesis and the characterization of a novel dinuclear complex of type $[(bpy)_2Ru\text{-}\mathbf{L3}\text{-}Ru(bpy)_2]^{2+}$, Ru(**L3**)Ru, where **L3** is the bis-anion derived from bis-2,3-(1,H-tetrazol-5-yl)pyrazine, is also reported.

Introduction

The coexistence of outstanding photophysical performances and favorable electrochemical properties have made polypyridyl complexes of d^6 metal ions such as Ru(II), Os(II), and Ir(III) one of the most popular classes of coordination compounds.[1] Applications for this kind of chemically stable molecules cover a wide range of research fields,[2] including the design of photosensitizers for light harvesting

* To whom correspondence should be addressed. E-mail: stefano.stagni@unibo.it (S.S.), palazzi@ms.fci.unibo.it (A.P.), decola@uni-muenster.de (L.D.C.).
† Dipartimento di Chimica Fisica ed Inorganica, Università di Bologna.
‡ Westfälische Wilhelms-Universität Münster.
§ Center for Nanotechnology.
|| Dipartimento di Chimica "G. Ciamician", Università di Bologna.

(1) (a) Balzani, V.; Scandola, F. *Supramolecular Photochemistry*; Ellis Horwood: Chichester, U.K., 1991. (b) Sauvage, J.-P.; Collin, J.-P.; Chambron, J.-C.; Guillerez, S.; Coudret, C.; Balzani, V.; Barigelletti, F.; De Cola, L.; Flamigni, L. *Chem. Rev.* **1994**, *94*, 993. (c) Balzani, V.; Juris, A. *Coord. Chem. Rev.* **2001**, *211*, 97.
(2) Vos, J. G.; Kelly, J. M. *Dalton Trans.* **2006**, 4869 and references therein.

10.1021/ic7011556 CCC: $37.00
Published on Web 09/29/2007

devices,[3] the synthesis of electrochemiluminescent (ECL) molecules,[4] DNA photoprobing,[5] and the most recent development, photoactive units for light-driven catalysis.[6] Since the light-emitting abilities and redox behaviors of these complexes are strongly ligand-dependent, a considerable research interest has been dedicated to the fine-tuning of those properties by varying the structure of the polypyridyls commonly employed.[1,2,7] In particular, the introduction of imydazolyl[8] or triazolyl[9] rings in the backbone of such ligands has led to a number of "polypyridine analogues", in which the multidentate character of the N-heterocycles allowed the modulation of the spectroscopic and redox properties of the resulting Ru(II) complexes by a pH-dependent mechanism.[8a,b,10] Despite their rarely being considered for the design of Ru(II)[11] or Os(II)[12] polypyridyl complexes, tetrazole-based compounds (R-CN_4H), which constitute a similar class of aromatic five-membered N-heterocycles, were recently shown to be interesting "actor" ligands for such molecular systems. For instance, the modification of the tpy ligand (tpy is 2,2′:6′,2″ terpyridine) by the introduction of tetrazolate moieties led to a Ru(II) complex showing enhanced photophysical performances with respect to those of the poorly luminescent $Ru(tpy)_2^{2+}$.[13] Furthermore, in one of our previous papers,[14a] we unexpectedly found that a dinuclear complex formed by two Ru(tpy)(bpy) units (bpy is 2,2′-bipyridyl) with a tetrazolate-bridging ligand exhibits an ECL response of magnitude comparable to that of $Ru(bpy)_3^{2+}$. These results prompted us to extend such studies by further exploiting the chelating tetrazolates as ligands for ruthenium(II) polypyridyl moieties. Herein, we report the synthesis and the photophysical and redox characterization of the $Ru(bpy)_2L$-type complexes (see Scheme 1) such as the model compound Ru**L1**[11b] (**L1** is the deprotonated form of 2-(*1,H*-tetrazol-5-yl)pyridine) and the novel pyrazinyl−tetrazolate complex Ru**L2**, as well as the study of the variation of their properties upon addition of a methyl group. Finally, we extend our studies to the preparation of the dinuclear species Ru(**L3**)Ru containing the novel bis-tetrazolate ligand $\mathbf{L3}^{2-}$, which might be considered as the bis-anionic analogue of the "popular" neutral ligand 2,3-bis(2-pyridyl)pyrazine, 2,3 dpp.[15]

Results and Discussion

Syntheses, NMR Characterization, and X-ray Diffraction Studies. The procedure adopted for the synthesis of the desired mono- and dinuclear complexes [Ru**L1**][PF_6], [Ru**L2**][PF_6], and [Ru(**L3**)Ru][PF_6]$_2$ (Scheme 2) involved the preliminary reaction of the ruthenium precursor *cis*-[Ru(bpy)$_2$$Cl_2$] with a slight molar excess (2.5 equiv) of a silver salt, such as $AgPF_6$, in refluxing ethanol. The removal of the precipitated AgCl afforded a deep-red filtrate, which was thoroughly combined with an ethanol solution of the desired 5-substituted tetrazolate ligand. The resulting reaction mixtures were heated at reflux temperature for 8−10 h, and the target compounds were purified via alumina-filled column chromatographies.

The confirmation of the composition of all complexes was provided by the positive ion electrospray ionization (ESI) mass spectra.

Mononuclear Complexes. The NMR characterization of the mononuclear species Ru**L1** and Ru**L2** was somewhat complicated by the low symmetry of the complexes and by the aromatic nature of the ligands. As a consequence, each ^1H and ^{13}C NMR spectrum (see Supporting Information, Figures S1 and S2) displays a number of resonances equal to the total number of aromatic protons or carbons in the complex. However, the unambiguous distinction of the resonances of the unsymmetrical tetrazolate ligands (see Table 1) from those due to inequivalent bpy rings has been achieved by the use of ^1H gs-COSY, ^1H,^{13}C gs-HSQC, and

(3) (a) Grätzel, M. *Inorg. Chem.* **2005**, *44*, 6841. (b) Meyer, G. J. *Inorg. Chem.* **2005**, *44*, 6852. (c) Biancardo, M.; Argazzi, R.; Bignozzi, C. A. *Inorg. Chem.* **2005**, *44*, 9619 and references therein.

(4) (a) Richter, M. M. *Chem. Rev.* **2004**, *104*, 3003. (b) Miao, W. J.; Bard, A. J. *Anal. Chem.* **2004**, *76*, 7109. (c) Welter, S.; Brunner, K.; Hofstraat, J. W.; De Cola, L. *Nature* **2003**, *421*, 54. (d) Liu, C.-Y.; Bard, A. J. *Acc. Chem. Res.* **1999**, *32*, 235 and references therein.

(5) (a) Erkkila, K. E.; Odom, D. T.; Barton, J. K. *Chem. Rev.* **1999**, *99*, 2777 and references therein. (b) Blasius, R.; Nierengarten, M.; Luhmer, M.; Constant, J. F.; Defrancq, E.; Dumy, P.; van Dorsselaer, A.; Moucheron, C.; Kirsch-De Mesmaeker, A. *Chem.—Eur. J.* **2005**, *11*, 1507. (c) van der Schindel, K.; Garcia, F.; Kooijman H.; Spek, A. L.; Haasnoot, J. G.; Reedijk, J. *Angew. Chem., Int. Ed.* **2004**, *43*, 5668.

(6) (a) Inagaki, A.; Yatsuda, S.; Edure, S.; Suzuki, A.; Takahashi, T.; Akita, M. *Inorg. Chem.* **2007**, *46*, 2432. (b) Rau, S.; Walther, D.; Vos, J. G. *Dalton Trans.* **2007**, 915 and references therein.

(7) (a) Medlycott, E. A.; Hanan, G. S. *Chem. Soc. Rev.* **2005**, *34*, 133. (b) Hofmeier, H.; Schubert, U. S. *Chem. Soc. Rev.* **2004**, *33*, 373. (c) Newkome, G. R.; Patri, A. K.; Holder, E.; Schubert, U. S. *Eur. J. Org. Chem.* **2004**, *2*, 235. (d) Elsevier, C. J.; Reedijk, J.; Walton, P. H.; Ward, M. D. *Dalton Trans.* **2003**, 1869. (e) Launay, J. P. *Chem. Soc. Rev.* **2001**, *30*, 386. (f) Balzani, V.; Juris, A.; Venturi, M.; Campagna, S.; Serroni, S. *Chem. Rev.* **1996**, *96*, 759 and references therein.

(8) (a) Han, M. J.; Gao, L. H.; Lu, Y. Y.; Wang, K. Z. *J. Phys. Chem. B* **2006**, *110*, 2364; (b) Haga, M.-A.; Takasugi, T.; Tomie, A.; Ishizuya, M.; Yamada, T.; Hossain, M. D.; Inoue, M. *Dalton Trans.* **2003**, 2069 and references therein. See also: (c) Hatzidimitriou, A.; Gourdon, A.; Devillers, J.; Launay, J. P.; Mena, E.; Amouyal, E. *Inorg. Chem.* **1996**, *35*, 2212.

(9) (a) Browne, W. R.; Hage, R.; Vos, J. G. *Coord. Chem. Rev.* **2006**, *250*, 1653. (b) Klingele, M. H.; Brooker, S. *Coord. Chem. Rev.* **2003**, *241*, 119. (c) Fanni, S.; Keyes, T. E.; O'Connor, C. M.; Hughes, H.; Wang, R.; Vos, J. G. *Coord. Chem. Rev.* **2000**, *208*, 77 and references therein.

(10) Di Pietro, C.; Serroni, S.; Campagna, S.; Gandolfi, M. T.; Ballardini, R.; Fanni, S.; Browne, W. R.; Vos, J. G. *Inorg. Chem.* **2002**, *41*, 2871 and references therein.

(11) (a) Massi, M.; Cavallini, M.; Stagni, S.; Palazzi, A.; Biscarini, F. *Mat. Sci. Eng., C* **2003**, *23*, 923. (b) Downard, A. J.; Steel, P. J.; Steenwijk, J. *Aust. J. Chem.* **1995**, *48*, 1625.

(12) (a) Demadis, K. D.; Meyer, T. J.; White, P. S. *Inorg. Chem.* **1998**, *37*, 3610. (b) Demadis, K. D.; El-Samanody, E.-S.; Meyer, T. J.; White, P. S. *Inorg. Chem.* **1998**, *37*, 838.

(13) Duati, M.; Tasca, S.; Lynch, F. C.; Bohlen, H.; Vos, J. G.; Stagni, S.; Ward, M. D. *Inorg. Chem.* **2003**, *42*, 8377;

(14) (a) Stagni, S.; Palazzi, A.; Zacchini, S.; Ballarin, B.; Bruno, C.; Marcaccio, M.; Paolucci, F.; Monari, M.; Carano, M.; Bard, A. J. *Inorg. Chem.* **2006**, *45*, 695. See also: (b) Zanarini, S.; Bard, A. J.; Marcaccio, M.; Palazzi, A.; Paolucci, F.; Stagni, S. *J. Phys. Chem. B* **2006**, *110*, 22551.

(15) (a) Marcaccio, M.; Paolucci, F.; Paradisi, C.; Roffia, S.; Fontanesi, C.; Yellowlees, L. J.; Serroni, S.; Campagna, S.; Balzani, V. *J. Am. Chem. Soc.* **1999**, *121*, 10081. (b) Marcaccio, M.; Paolucci, F.; Paradisi, C.; Carano, M.; Roffia, S.; Fontanesi, C.; Yellowlees, L. J.; Serroni, S.; Campagna, S.; Balzani, V. *J. Electroanal. Chem.* **2002**, *532*, 99. (c) Marcaccio, M.; Paolucci, F.; Fontanesi, C.; Fioravanti, G.; Zanarini, S. *Inorg. Chim. Acta* **2007**, *360*, 1154. (d) Puntoriero, F.; Serroni, S.; Galletta, M.; Juris, A.; Licciardello, A.; Chiorboli, C.; Campagna, S.; Scandola, F. *ChemPhysChem* **2005**, *6*, 129 and references therein.

Scheme 1. Ligands, Complexes, and Acronyms Used in This Work

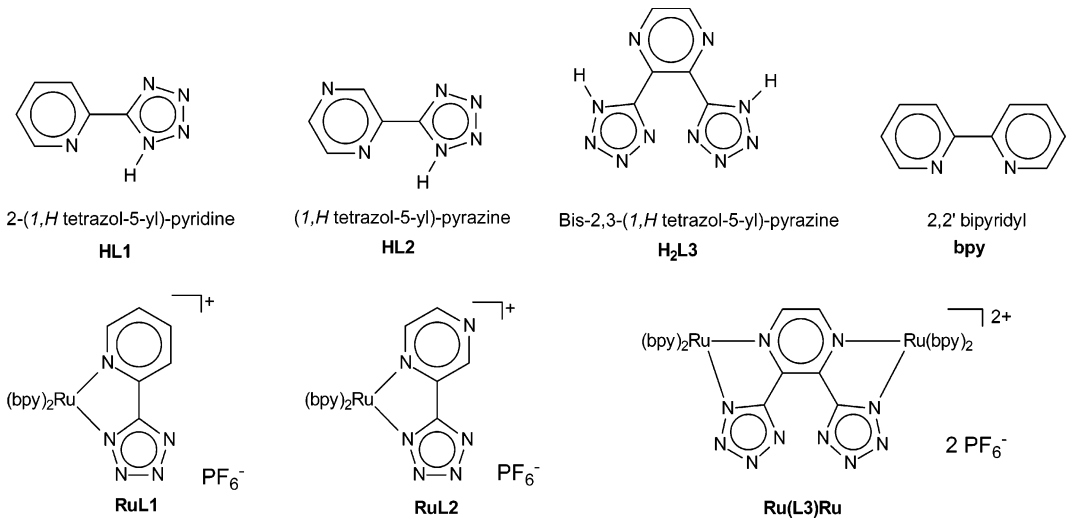

Scheme 2. Synthetic Procedure for the Preparation of the Target Complexes

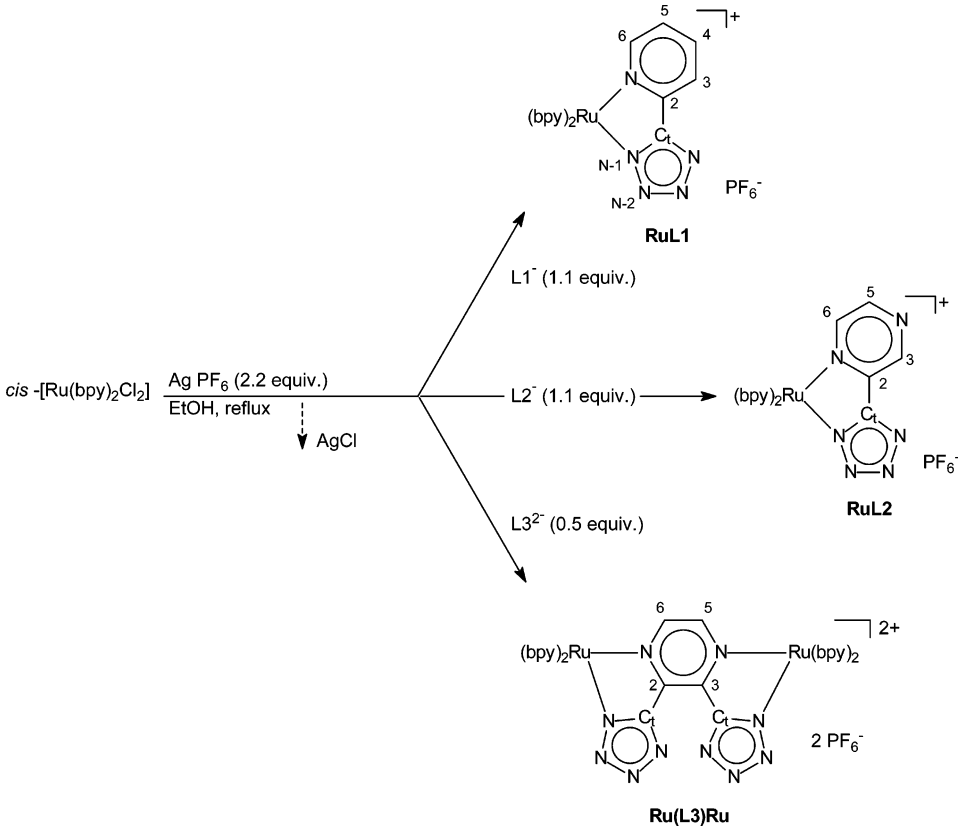

^{1}H,^{13}C gs-HMQC two-dimensional techniques. Even though the NMR experiments were performed in different solvents ($(CD_3)_2SO$ for the ligands and CD_3CN for the corresponding complexes), the comparison of the ^{1}H NMR data of complexes Ru**L1** and Ru**L2** with those of the corresponding "free" ligands (see Table 1) indicates that the coordination of the tetrazolate moiety to the ruthenium center results in a pronounced upfield shift (more than 1.0 ppm) of the H6 proton (see Scheme 2 for atom numbering), while the remaining resonances are almost unchanged. A similar behavior is in perfect agreement with that previously described for analogous or closely related $[Ru(bpy)_2L]^+$ species.[11b,16]

Some structural and electronic features of the coordinated tetrazolate moieties are deducible from the analysis of the ^{13}C NMR spectra of the corresponding mononuclear species. Indeed, as previously reported for metal complexes containing monocoordinated 5-aryl tetrazolates,[14,17] the tetrazole carbon (Ct) resonance is a reliable parameter to determine which of the two inequivalent tetrazole nitrogens binds to the metal. (Scheme 3)

In particular, the formation of N-1 coordination isomers is witnessed by the Ct resonating in the chemical shifts range

(16) Browne, W. R.; O'Connor, C. M.; Hughes, H. P.; Hage, R.; Walter, O.; Doering, M.; Gallagher, J. F.; Vos, J. G. *Dalton Trans.* **2002**, 4048.

Table 1. Selected ^{1}H (400 MMz) and ^{13}C (100 MMz) NMR Data of All the Ligands[a] and Complexes[b] Reported in This Paper[f]

entry	δC_t	δH_3	δC_3	δH_4	δC_4	δH_5	δC_5	δH_6	δC_6
H**L1**	154.9	8.19	122.7	8.04	138.3	7.59	126.1	8.76	150.1
Ru**L1**	162.9	8.27	123.0	7.97[c]	138.9	7.33	126.6	7.56	152.5
Ru**L1**Me	166.1	8.39	124.6	8.05[c]	139.9	7.36	129.7	7.77	153.7
H**L2**	153.5	9.37	143.3			8.85	146.8	8.85	144.8
Ru**L2**	161.2	9.42	143.6			8.39	147.3	7.69	146.8
Ru**L2**Me	164.7	9.50	145.3			8.59	149.9	7.80	148.5
H**L3**	153.4		139.8			9.09	146.1	9.09	146.1
Ru(**L3**)Ru[d]	161.5		146.2			7.30[e]	146.6	7.31[e]	146.6

[a] Dimethylsulfoxide-d_6 as solvent, at r.t. [b] CD_3CN as solvent, at r.t.; chemical shifts are expressed in ppm. [c]Overlapping with bpy resonances; [d] Unseparated mixture of diastereomers; the chemical shifts are relative to the signals showing higher intensity. [e] Spectrum recorded at r.t. with a Varian Inova 600 MHz instrument. [f] See Scheme 2 for atom labeling.

Scheme 3. N-1 and N-2 Coordination Isomers of Tetrazolate Complexes

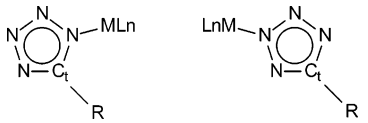

N-1 isomer N-2 isomer

between 151 and 155 ppm, while the less hindered N-2 isomers typically show a downfield-shifted (161−165 ppm) Ct signal. It is therefore surprising that the tetrazole carbon resonances of the mononuclear complexes Ru**L1** and Ru**L2** are found at 163 and 161 ppm, respectively, even though from the crystal structure analysis it emerges that the tetrazole ring is formally N-1 (labeled as N-6 in the crystal structures; see further on in Figures 1, 3, and 4) coordinated to the metal center. This anomalous behavior can be explained by considering that the coordination geometry forces the aromatic rings of the tetrazolate ligand to adopt a coplanar arrangement, giving rise to a significant interannular conjugation effect.[17a−c,18] These hypotheses are supported by the molecular structure of Ru**L2** in its [Ru**L2**][PF_6]·0.5Et_2O·0.5H_2O salt (Figure 1 and Table 2). As a consequence of the coordination of **L2** to the metal, the pyrazyl and tetrazole rings are almost perfectly coplanar (torsion angles N(5)−C(25)−C(26)−N(6) 0.5(6)°; C(24)−C(25)−C(26)−N(9) −2.2-(9)°). The Ru−N distances with the two bpy ligands are in the normal range for this type or Ru(II) complexes.[16,19] Considering the chelating pyrazyl−tetrazolate ligand, the corresponding Ru−N distances (Ru(1)−N(5) 2.085(4) Å; Ru-(1)−N(6) 2.040(4) Å) display a considerable asymmetry, with the interaction between the Ru center and the pyrazine ring quite long. A similar behavior has been observed in the related $[Ru(bpy)_2(cept)]^+$ complex (cept = 3-(ethoxycarbonyl)-5-(pyrid-2′-yl)-1,2,4-triazolate)[19] and ascribed to the limited π backbonding of the pyridyltriazole-containing

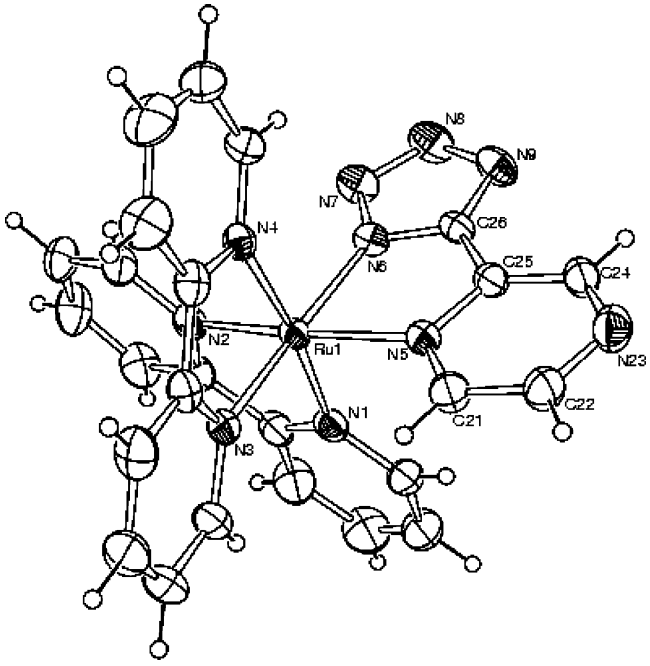

Figure 1. Molecular structure of Ru**L2**, with key atoms labeled. Displacement ellipsoids are at the 30% probability level.

Table 2. Selected Bond Lengths (Å) and Angles (deg) for Ru**L2**, Ru**L1**Me, and Ru**L2**Me

	Ru**L2**	Ru**L1**Me	Ru**L2**Me
Ru(1)−N(1)	2.057(4)	2.062(3)	2.069(3)
Ru(1)−N(2)	2.048(4)	2.046(3)	2.060(3)
Ru(1)−N(3)	2.056(4)	2.061(3)	2.051(3)
Ru(1)−N(4)	2.063(4)	2.063(3)	2.064(3)
Ru(1)−N(5)	2.085(4)	2.104(3)	2.076(3)
Ru(1)−N(6)	2.040(4)	2.048(3)	2.059(3)
N(6)−N(7)	1.349(6)	1.319(4)	1.327(4)
N(7)−N(8)	1.305(7)	1.322(5)	1.320(4)
N(8)−N(9)	1.353(7)	1.337(5)	1.329(4)
N(9)−C(26)	1.328(6)	1.321(5)	1.320(4)
C(26)−N(6)	1.325(6)	1.345(5)	1.353(4)
C(25)−C(26)	1.442(7)	1.450(5)	1.449(5)
N(6)−N(7)−N(8)	107.1(4)	104.6(3)	104.1(3)
N(7)−N(8)−N(9)	111.2(4)	114.4(3)	115.7(3)
N(8)−N(9)−C(26)	103.9(4)	101.6(3)	100.8(3)
N(9)−C(26)−N(6)	111.2(4)	111.8(3)	112.5(3)
C(26)−N(6)−N(7)	106.6(4)	107.6(3)	106.9(3)

ruthenium(II) complexes. The water molecule in the [Ru**L2**]-[PF_6]·0.5Et_2O·0.5H_2O salt forms hydrogen bonds with the tetrazolate rings of two neighboring Ru**L2** cations (O(2)−H(1O)···N(9)#2: d(D−H) 0.83(2) Å; d(H···A) 2.61(8) Å; d(D···A) 3.021(7) Å; DHA 112(7)°; symmetry operation #2, $x + 1, -y + 1, z + {}^1/_2$).

Addition of Electrophiles. The presence of three imine-type nitrogens in the coordinated tetrazole moiety gives the possibility of performing electrophilic additions onto the corresponding mononuclear complexes. The treatment of complexes Ru**L1** and Ru**L2** with 1 equiv of methyl triflate led to the formation of the bis-cationic compounds Ru**L1**Me and Ru**L2**Me, which were isolated as their PF_6^- salts after an anion-exchange procedure (Scheme 4).

The ^{1}H NMR spectra of the methylated species are consistent with the formation of monomethylated products, as evidenced by the presence of one methyl singlet at ca.

(17) (a) Palazzi, A.; Stagni, S. *J. Organomet. Chem.* **2005**, *690*, 2052. (b) Palazzi, A.; Stagni, S.; Monari, M.; Selva, S. *J. Organomet. Chem.* **2003**, *669*, 135. (c) Palazzi, A.; Stagni, S.; Bordoni, S.; Monari, M.; Selva, S. *Organometallics* **2002**, *21*, 3774. (d) Jackson, W. G.; Cortez, S. *Inorg. Chem.* **1994**, *33*, 1921 and references therein.

(18) Butler, R. N. In *Comprehensive Heterocyclic Chemistry II, Tetrazoles*; Storr, R. C., Ed.; Pergamon Press, Oxford, 1996; Vol. 4, pp 621−678 and references therein.

(19) Mehmetaj, B.; Haasnoot, J. G.; De Cola, L.; van Albada, G. A.; Mutikainen, I.; Turpeinen, U.; Reedijk, J. *Eur. J. Inorg. Chem.* **2002**, *7*, 1765 and references therein.

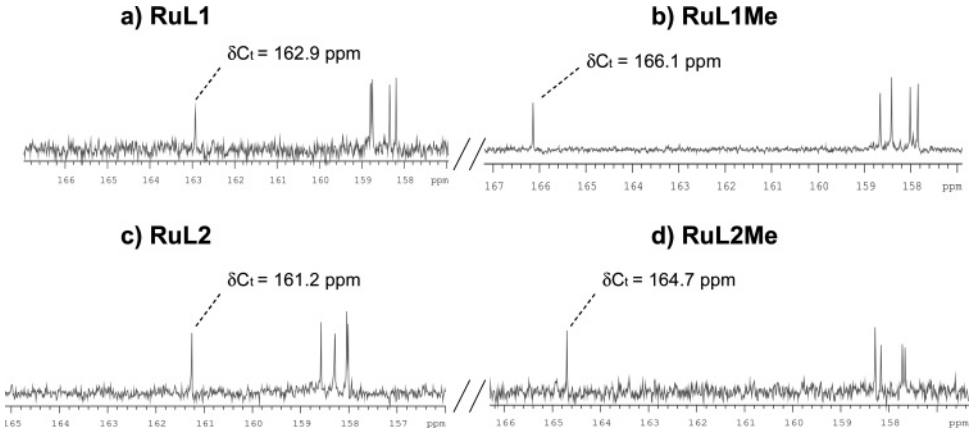

Figure 2. Downfield shifting of Ct resonance upon methylation of (a) Ru**L1** and (c) Ru**L2**.

Scheme 4. General Procedure for the Methylation of Mononuclear Complexes

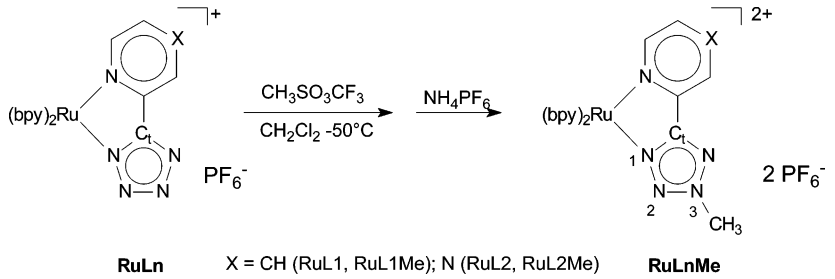

4.2 ppm (Figures S3a and S4a, Supporting Information). Further hypothesis about the structure of the complexes can be made on the basis of the ^{13}C NMR features. As for example, the ^{13}C NMR spectrum of the pyridyl−tetrazolate methylated complex Ru**L1**Me displays a single Ct resonance at 166.1 ppm (Figure 2a).

This signal is significantly downfield shifted (ΔCt = (δCt$_{\mathrm{RuL1Me}}$ − δ Ct$_{\mathrm{RuL1}}$) = 3.1 ppm) with respect to that of the starting compound Ru**L1**, while the remaining resonances do not change in such an appreciable way. A similar variation of the Ct resonance, together with the presence of a single Ct signal (see Figure 2a,b), indicate that methylation takes place to the tetrazole ring and also occurs regioselectively on the nitrogen N-3 atom (see Scheme 4 for atom numbering), the one which suffers less from steric hindrance. An analogous behavior is observed when the pyrazyl−tetrazolate complex Ru**L2** is treated with 1 equiv of methyl triflate (Figure 2c,d). In this case, the ^{13}C NMR spectrum of the resulting methylated species Ru**L2**Me (ΔCt = (δCt$_{\mathrm{RuL2Me}}$ − δ Ct$_{\mathrm{RuL2}}$) = 3.3 ppm) indicates that the addition of the methyl group chemoselectively occurs on the tetrazole moiety. The crystal structures of Ru**L1**Me and Ru**L2**Me are shown in Figures 3 and 4, respectively, whereas selected bond lengths and angles are reported in Table 2. Unequivocally, in both cases methylation occurs on the N-3 atom (labeled as N-8 in the crystal structures shown in Figures 3 and 4) and does not cause any major variation in the bonding parameters of the complexes compared to the non-methylated species Ru**L2**. In particular, the pyrazine and tetrazole rings retain their coplanarity (torsion angles N(5)−C(25)−C(26)−N(6) 0.0(5)° and C(24)−C(25)−C(26)−N(9) 2.0(9)° for Ru**L1**Me; N(5)−C(25)−C(26)−N(6) −4.0(4)° and C(24)−C(25)−C(26)−N(9) −3.6(6)° for Ru**L2**Me).

Dinuclear Complex Ru(L3)Ru. The dinuclear species Ru(**L3**)Ru was isolated as a mixture of the homochiral rac ($\Delta\Delta/\Lambda\Lambda$) and the heterochiral meso ($\Delta\Lambda/\Lambda\Delta$) diastereoisomers, as confirmed by ^{13}C NMR and, more clearly, by ^{1}H NMR analysis in solution. In the first case, the spectrum (Figure S5, Supporting Information) showed the partial overlap of two differently intense patterns of 23 peaks, while in the ^{1}H NMR spectrum there is neat evidence of two closely spaced signals (δHa = 7.306 ppm and δHb = 7.311 ppm; see Figure 5) representing the pyrazine ring protons (H5 and H6; see Scheme 2) of each diastereomeric form. Furthermore, their different intensities (integral ratio Ha/Hb = ca. 2/1) suggested the prevalence of one isomer over the other.

Concerning the ^{13}C NMR spectrum (Figure S5, Supporting Information), Ru(**L3**)Ru displays well-resolved signals of the bis-tetrazolate linker as a Ct signal at 161.5 ppm, while the remaining bridging ligand resonances are found in a "bpy-free" region of the spectra at 146.6 (C5 and C6, see Scheme 1) and 146.2 (C2 and C3) ppm, respectively. However, the sole NMR evidence was not sufficient to unambiguously attribute the predominant signals to the meso or to the rac forms.[20] Indeed, despite our efforts, we did not succeed in the isolation of the pure diastereomers. In addition (see also, Experimental Section), at the end of the purification process the dinuclear complex Ru(**L3**)Ru was found to be accompanied by a presumably trinuclear impurity, whose

(20) Keene, R. F. *Chem. Soc. Rev.* **1998**, *27*, 185 and references therein. For some recent papers about similar dinuclear species see: (a) D'Alessandro, D. M.; Dinolfo, P. H.; Davies, M. S.; Hupp, J. T.; Keene, F. R. *Inorg. Chem.* **2006**, *45*, 3261 and references therein. (b) Browne, W. R.; O'Boyle, N. M.; Henry, W.; Guckian, A. L.; Horn, S.; Fett, T.; O'Connor, C. M.; Duati, M.; De Cola, L.; Coates, C. G.; Ronayne, K. L. McGarvey, J. J.; Vos, J. G. *J. Am. Chem. Soc.* **2005**, *129*, 1229.

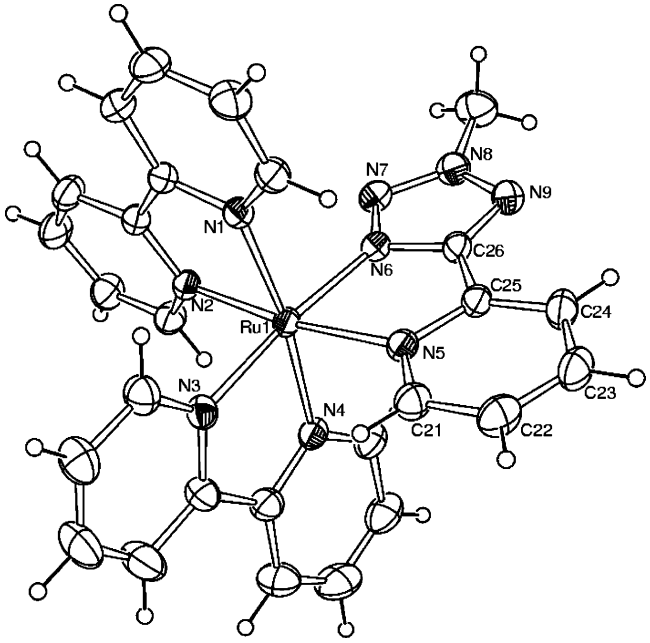

Figure 3. Molecular structure of Ru**L1**Me, with key atoms labeled. Displacement ellipsoids are at the 30% probability level.

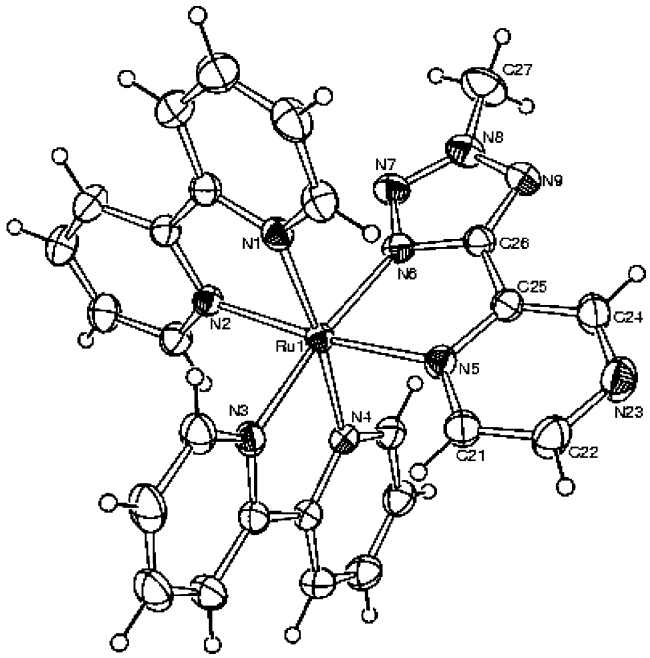

Figure 4. Molecular structure of Ru**L2**Me, with key atoms labeled. Displacement ellipsoids are at the 30% probability level.

presence could not be avoided even with repeated column chromatographies. Since attempts for the purification of Ru(**L3**)Ru are being currently pursued in our laboratories, we prefer to fully report on its electrochemical and photophysical properties later.

Redox Properties. The redox behavior of the complexes was investigated in acetonitrile solution by cyclic voltammetry (CV), at room temperature. All potentials are collected in Table 3. In the region of the positive potentials, all the mononuclear species exhibited a single one-electron reversible process, which can be confidently attributed to the oxidation of the Ru(II) center. As expected, the oxidation of the pyrazinyl−tetrazolate complex Ru**L2** is found to occur at more positive potentials than that of the homologue pyridyl-based Ru**L1**. This is due to the better electron-withdrawing character of the pyrazine ring of **L2**, which yields weaker σ-donor and stronger π-acceptor properties, compared with those of the pyridine ligand. Concerning the reductions, the voltammetric investigation has been carried out by exploring the first processes and in particular those occurring within the potential window down to −2.0 V. The mononuclear species Ru**L1** (Figure 6a) and Ru**L2** (Figure S6a, Supporting Information) both show two completely reversible one-electron reductions. The first process occurs at nearly the same potential (10 mV difference with Ru**L2**, easier to be reduced) for both species whereas for the second reduction the pyrazinyl−tetrazolate complex Ru**L2** is reduced at a potential that is 90 mV less negative than that of Ru**L1**. Such a difference can be accounted for by the better electron π-acceptor properties of the pyrazinyl **L2** ligand with respect to **L1**, and hence, the interligand interactions for the former ligand are less intense than those observed for the complex containing the latter ligand. Thus, on the basis of these findings, together with the known electronic properties of previously investigated polypyridine species,[14,15a,b] the two reductions can be attributed to the two bpy ligands. Furthermore, the formal negative charge brought by the tetrazolate ligands makes their reductions more difficult and to be expected outside the negative limit of the explored potential window.[14a] In order to further support the assignment of the reductions, as discussed above, the investigation of the two corresponding tetrazole methylated complexes Ru**L1**Me (see Figure 6b) and Ru**L2**Me (Figure S6b), respectively, was carried out. The methylation moves the tetrazole-centered reduction within our experimental potential window, making the ligand itself the most easily reduced species. As a consequence, the two bpy processes shift to more-negative potentials, keeping the inter-bpy interaction substantially at the same magnitude. The increased charge of the methylated complexes is also responsible for the positive shift of the Ru-centered oxidation processes compared with those of the corresponding Ru**L1** and Ru**L2** complexes. Notice that the small voltammetric peak at about 1.0 V in the voltammetric curve of the Ru**L1**Me complex (Figure 6b) is due to the small amount of Ru**L1** present as an impurity (see also Experimental Section).

Electronic Spectroscopy. In Figure 7, we report the absorption spectra of all complexes recorded in acetonitrile solutions. The spectra show the expected features of most Ru-based metal complexes[21] with intense transitions at high energy (200−350 nm) and weaker bands in the visible region (400−600 nm). The series of bands in the UV range (ϵ = 18−90 × 10^3 M^{-1} cm^{-1}) can be assigned to ligand-centered bpy-based $\pi \rightarrow \pi^*$ (^{1}LC) absorptions. The features observed in the visible part of the spectrum (ϵ = 5−20 × 10^3 M^{-1} cm^{-1}) are assigned to singlet and triplet metal-to-ligand

(21) (a) Hage, R.; Prins, R.; Haasnoot, J. G.; Reedijk, J.; Vos, J. G. *J. Chem. Soc., Dalton Trans.* **1987**, 1389. (b) Nieuwenhuis, H. A.; Haasnoot, J. G.; Hage, R.; Reedijk, J.; Snoeck, T. L.; Stufkens, D. J.; Vos, J. G. *Inorg. Chem.* **1991**, *30*, 48. (c) Hage, R.; Dijkhuis, A. H. J.; Haasnoot, J. G.; Prins, R.; Reedijk, J.; Buchanan, B. E.; Vos, J. G. *Inorg. Chem.* **1988**, *27*, 2185. (d) De Cola, L.; Belser, P. *Coord. Chem. Rev.* **1998**, *177*, 301 and references therein.

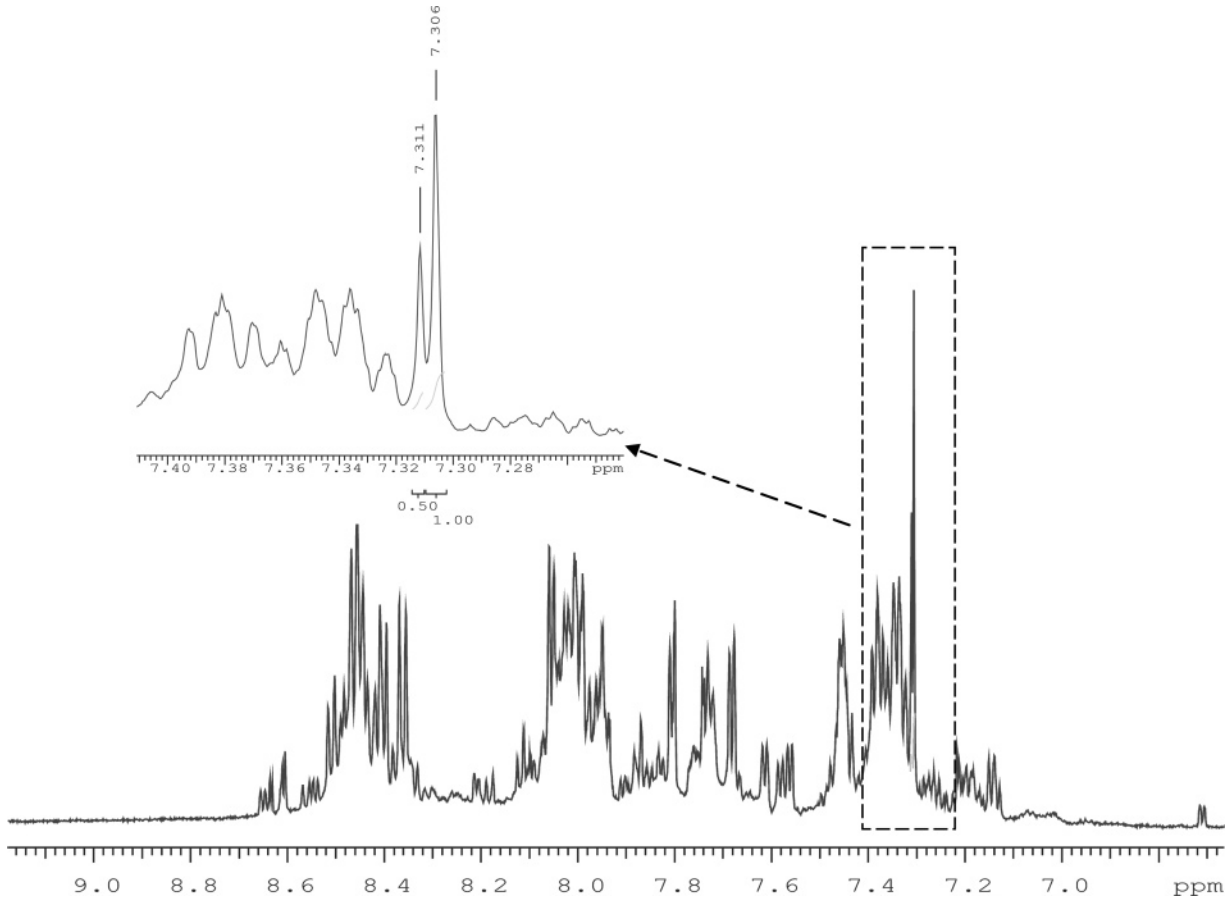

Figure 5. ^{1}H NMR spectrum of Ru(**L3**)Ru as a mixture of meso (ΔΛ/ΛΔ) and rac (ΔΔ/ΛΛ) diastereomers.

Table 3. Half-Wave ($E_{1/2}$) Redox Potentials[a] (versus SCE) of All Complexes at 25 °C

		(red) − $E_{1/2}$/V		
entry	(ox) − $E_{1/2}$/V			
Ru**L1**	1.03	−1.40	−1.70	
Ru**L1**Me	1.41	−1.34	−1.55	−1.89
Ru**L2**	1.20	−1.39	−1.61	
Ru**L2**Me	1.52	−1.12	−1.48	−1.72

[a] In 0.05 M TBAH/acetonitrile solution.

charge transfer (^{1}MLCT) transitions, involving Ru → bpy and Ru → L transitions. In this region, the mononuclear complexes show a strong overlapping of two broad bands at about 420 and 440 nm. The photophysical data of the studied complexes, with the exception of Ru(**L3**)Ru, are collected in Table 4.

All complexes are luminescent in acetonitrile at 298 K, and the emission spectra are reported in Figure 8. The broad structure of these emission bands and their energy range (600−850 nm) are typical for ^{3}MLCT-based emission of ruthenium polypyridyl complexes.[16,21d] The large blue shift observed on going from 298 to 77 K is also in agreement with this assignment. The phosphorescence character of such emissions is also proved by their extreme oxygen sensitivity, which almost completely quenches the already weak emissive process. Interestingly, replacement of the pyridine ring in Ru**L1** for a pyrazine ring in complex Ru**L2** results in a dramatic reduction in emission intensity and excited-state lifetimes (τ), together with a blue shift in emission energy.

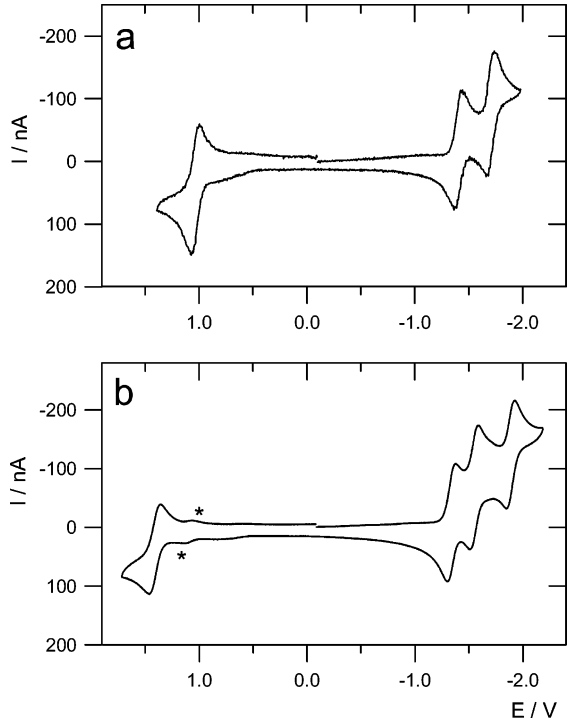

Figure 6. Cyclic voltammetric curves of mononuclear complexes: (a) 1 mM Ru**L1** in a 0.06 M TBAH/ACN solution; working electrode Pt disk, diameter = 125 μm; T = 25 °C; scan rate = 1 V/s; (b) 1 mM Ru**L1**Me in a 0.06 M TBAH/ACN solution; working electrode Pt disk, diameter = 125 μm; T = 25 °C; scan rate = 1 V/s. The symbol * in the voltammetric curve of Ru**L1**Me indicates the redox process due to small amounts of the starting compound Ru**L1** present as an impurity.

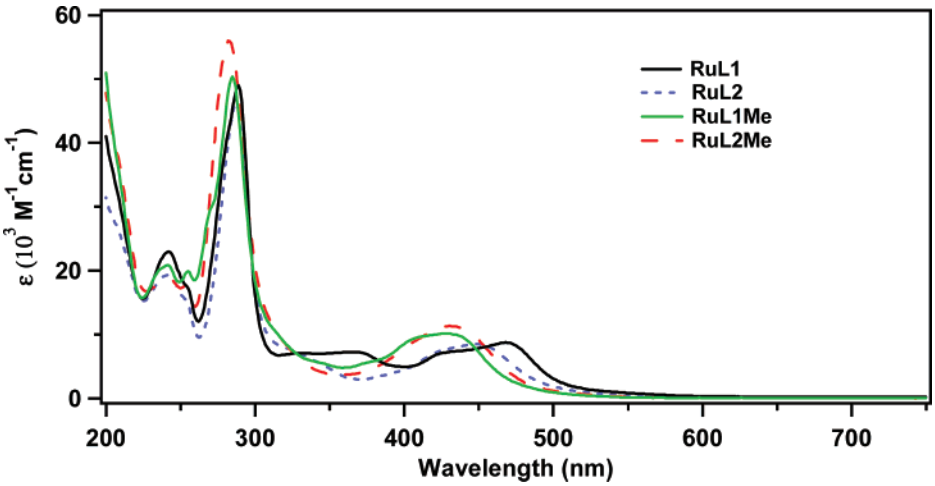

Figure 7. Absorption spectra in acetonitrile solutions at room temperature.

Table 4. Absorption and Emission Spectral Data of All the Complexes

	absorption[a]		emission, 298 K[d]					emission, 77 K[d]	
complex	λ/nm	ϵ /M^{-1} cm^{-1}	$\lambda_{max}{}^{a}$/nm	τ^{a}/ns	τ^{b}/ns	$\phi^{a}(10^{-3})$	$\phi^{b}(10^{-3})$	$\lambda_{max}{}^{c}$/nm	τ^{c}/μs
Ru**L1**	244	22 600	653	77	220	-	4	597	5.23
	289	49 000							
	367	7200							
	432	7270							
	468	8700							
Ru**L2**	244	19 000	646	5	6		0.3	582	6.59
	287	45 800							
	429	7600							
	447	8400							
Ru**L1**Me	242	20 800	644	71(67) 148(33)	160(10) 826(90)		1	557	7.1
	285	50 300							
	327	7100							
	410	9500							
	430	10 100							
Ru**L2**Me	242	18 700	617	150	820	3	21	580	10.7
	282	55 900							
	320	8500							
	410	9000							
	430	11 200							

[a] In air-equilibrated acetonitrile. [b] In degassed acetonitrile. [c] In butyronitrile glass. [d] λ_{ex} = 450 nm; for the biexponential excited-state lifetimes (τ), the relative weights of the exponential curves are reported in parentheses.

This bathochromic effect, as already mentioned, is related to the lower σ-donor strength and greater π-acceptor properties of pyrazine,[9a] which respectively induce a decrease in energy of the highest-occupied molecular orbital (HOMO) and the lowest-unoccupied molecular orbital (LUMO) levels of the complex; however, the HOMO level undergoes a bigger decrease than the LUMO level, thus enhancing the HOMO−LUMO gap. Such behavior is supported by the electrochemical data for the mononuclear complexes: As can be seen in Table 3, on going from Ru**L1** to Ru**L2**, the oxidation potentials increase 0.17 V, while the first reduction potential is negatively shifted by only 0.01 V. At low temperature, the shift of the MLCT band at much higher energies and the lack of thermal population of the triplet metal-centered (^{3}MC) state prevent efficient quenching. The long excited-state lifetime decays measured at low temperatures (in the microsecond range) also indicate that, at room temperature, population of the ^{3}MC is always occurring in all complexes, and in particular for Ru**L2**, which shows the strongest emission quenching.

As already observed for the case of our previously reported Ru(II)−tetrazolate complexes,[14a] upon the addition of a methyl group on the tetrazole ring of Ru**L1** and Ru**L2**, the emission maxima undergo a slight blue shift, more remarkable for Ru**L2**Me (∼30 nm) than for Ru**L1**Me (∼ 9 nm). Methylation results into higher energetic emission, since the addition of an electrophile likely leads to stabilization of the HOMO level, thus increasing the HOMO−LUMO gap. Concerning the emission lifetimes (τ), the highest values are displayed by the methylated derivatives Ru**L1**Me (the biexponential decay of which is probably due to the presence of some unreacted Ru**L1**) and Ru**L2**Me. It is worth noting that in this latter case, the excited-state lifetime at room temperature increases more than 10 times on going from the nearly nonemissive Ru**L2** to the methylated Ru**L2**Me (see Table 4). We cannot clearly elucidate the reasons for this effect, neither by considering the data reported by Vos and co-workers on the protonation of similar 1,2,4 triazolate Ru(II) complexes[10,16] nor by recalling the energy-gap law.[22] Nevertheless, as we have already reported,[14a,17a−c] the alky-

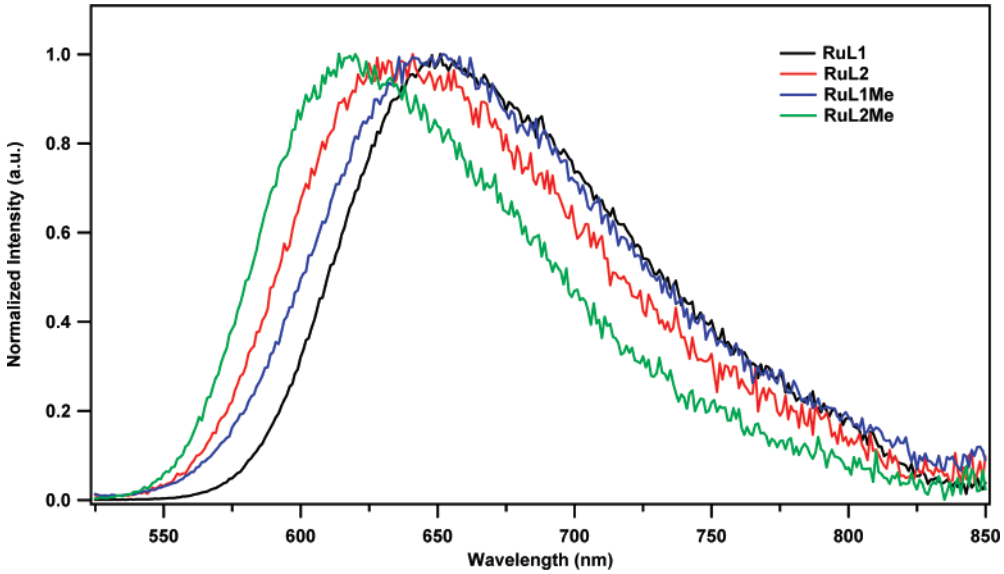

Figure 8. Normalized room-temperature emission spectra of all the complexes in acetonitrile solutions (λ_{exc} = 450 nm).

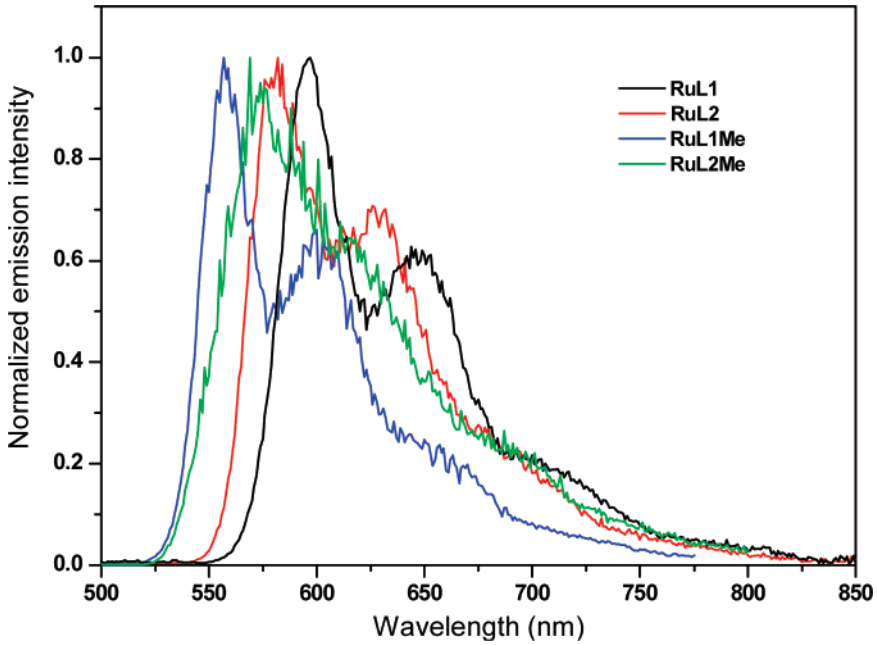

Figure 9. Normalized emission spectra recorded in butyronitrile glass at 77 K (λ_{exc} = 450 nm).

lation of coordinated tetrazolates is likely responsible not only for changes in the ligand σ-donor strength, but also for remarkable variations in the tetrazolate π-interannular conjugation. Therefore, on the basis of these considerations, we suspect that the latter feature might represent an important factor in determining a similar increase of excited-state lifetime values. The emission spectra recorded at 77 K for all the complexes were normalized and are reported in Figure 9. All emission spectra undergo to a blue shift if compared with those recorded at room temperature, and they all show more structured shapes.

Conclusions

In this paper, we report on our studies of pyridyl−tetrazolate or pyrazinyl−tetrazolates as anionic bpy-type ligands for Ru(II) polypyridyl complexes. The choice of a similar kind of "actor" ligands is first explained by considering their ease of preparation, which could also be pursued by a "click chemistry" procedure.[23] Then, at odds with the analogous 1,2,4-triazolate ligands, the symmetrical nature of the tetrazolate ring does not involve the formation of any coordination isomers. In addition, the geometrical and electronic features of the coordinated tetrazolates are clearly deducible from the ^{13}C NMR data of the resulting complexes. NMR spectroscopy is also an important tool to understand the reactivity of such compounds. Indeed, the chemo- and regioselectivity of electrophilic additions onto tetrazolate

(22) Durham, B.; Caspar, V. J.; Nagle, J. K.; Meyer, T. J. *J. Am. Chem. Soc.* **1982**, *104*, 4803.
(23) (a) Demko, Z. P.; Sharpless, K. B. *Angew. Chem., Int. Ed.* **2002**, *41*, 2110. (b) Demko, Z. P.; Sharpless, K. B. *Angew. Chem., Int. Ed.* **2002**, *41*, 2113.

complexes can be deduced on the basis of their ^{13}C NMR spectra and further corroborated by the X-ray structures of pyrazinyl−tetrazolate complexes Ru**L2** and Ru**L2**Me, together with the methylated pyridyl−tetrazolate complex Ru**L1**Me. It is worth noting that the simple addition of electrophilic species onto Ru**L1** and Ru**L2** also determines the significant variation of their electrochemical properties and, particularly, of their light-emission performances. As a matter of fact, the methylated derivatives Ru**L1**Me and Ru**L2**Me display longer emission lifetimes than those of the corresponding precursors Ru**L1** and Ru**L2**, the latter being poorly luminescent at room temperature. In general, the "sensitivity" toward the presence of electrophilic species shown by these Ru(II)−tetrazolate complexes might constitute a promising feature for the development (i.e., further complexation of coordinated tetrazolates) of such compounds and for their possible applications as chemosensors. Finally, we reported the first dinuclear complex of the type $[(bpy)_2Ru(\mathbf{L3})Ru(bpy)_2]$, Ru(**L3**)Ru, where **L3** is the deprotonated form of 2,3-bis(*1,H*-tetrazol-5-yl)-pyrazine. Since this dinuclear species was isolated as an unseparated mixture of meso ($\Delta\Lambda/\Lambda\Delta$) and rac ($\Delta\Delta/\Lambda\Lambda$) diastereoisomers together with other byproducts, we will report in a successive paper on the electrochemical and photophysical features of Ru(**L3**)Ru, as we are currently engaged in the preparation of pure products.

Experimental Section

Materials. Solvents were dried and distilled under nitrogen prior to use. Unless otherwise stated, chemicals were obtained commercially (e.g., Aldrich) and used without any further purification. *cis*-$Ru(bpy)_2Cl_2$ was prepared according to procedure of Sullivan and Meyer.[24] Throughout this paper, the percentage yields of the product complexes are referred to the molar quantity of the starting *cis*-$Ru(bpy)_2Cl_2$ compound. The atom numbering used for the description of NMR spectra (see below) is always referred to Scheme 2.

Warning! *Nitrogen-rich compounds such as tetrazole derivatives are used as components for explosive mixtures.[18] In this lab, the reactions described here were run on only a few grams scale, and no problems were encountered. However, great caution should be exercised when handling or heating compounds of this type.*

Instrumentation and Procedures. All the obtained complexes were characterized by elemental analysis and spectroscopic methods. Elemental analyses were performed on a ThermoQuest Flash 1112 Series EA instrument. ESI-mass spectra were performed on a Waters ZQ-4000 instrument; acetonitrile was used as the solvent. The routine NMR spectra (^1H, ^{13}C) were always recorded using a Varian Mercury Plus 400 instrument (^1H, 400.1 MHz; ^{13}C, 100 MHz), with the exception of the ^1H NMR analyses of the dinuclear complex Ru(**L3**)Ru, which were performed by using a Varian Inova 600 MHz instrument. The spectra were referenced internally to residual solvent resonance and were recorded at 298 K for characterization purposes. Bidimensional $^1H,^{13}C$ correlation spectra were measured via gs-HSQC and gs-HMBC experiments,[25] whereas $^1H,^1H$ correlations were determined by gs-COSY experiments.[26]

Electrochemistry. Tetrabutylammonium hexafluorophosphate (TBAH; from Fluka), as supporting electrolyte, was used as received. Dry acetonitrile (ACN), after being refluxed over CaH_2, was distilled under vacuum at room temperature (r.t.) with a high refluxing ratio, utilizing a 1 m length distillation column filled with glass rings, and it was stored in a special designed Schlenk flask over 3 Å activated molecular sieves, protected from light. Shortly before performing the experiment, the solvent was distilled via a closed system into an electrochemical cell containing the supporting electrolyte and the species under examination. Electrochemical experiments were carried out in an airtight single-compartment cell described elsewhere[15a] by using platinum working and counter electrodes and a silver spiral as a quasi-reference electrode. The cell containing the supporting electrolyte and the electroactive compound was dried under vacuum at 100−110 °C for at least 60 h before each experiment. All the $E_{1/2}$ potentials have been directly obtained from CV curves as averages of the cathodic and anodic peak potentials for one-electron peaks and by digital simulation for those processes closely spaced in multielectron voltammetric peaks. The $E_{1/2}$ values referred to an aqueous saturated calomel electrode (SCE) and have been determined by adding, at the end of each experiment, ferrocene as an internal standard and measuring them with respect to the ferrocinium/ferrocene couple standard potential.

Voltammograms were recorded either with a EcoChemie PG-STAT 20 system or an AMEL model 552 potentiostat controlled by an AMEL model 568 programmable function generator. The potentiostat was interfaced to a Nicolet model 3091 digital oscilloscope, and the data was transferred to a personal computer by the program *Antigona*.[27] The minimization of the uncompensated resistance effect in the voltammetric measurements was achieved by the positive-feedback circuit of the potentiostat.

Photophysics. Absorption spectra were measured on a Varian Cary 5000 double-beam UV−vis−NIR spectrometer and were baseline corrected. Steady-state emission spectra were recorded on a Spex Fluorolog 1681 equipped with a 150 W xenon arc lamp, single excitation and emission monochromators, and a Hamamatsu R928 photomultiplier tube or a HORIBA Jobin-Yvon IBH FL-322 Fluorolog 3 spectrometer equipped with a 450 W xenon arc lamp, double-grating excitation and emission monochromators (2.1 nm/mm dispersion; 1200 grooves/mm), and a Hamamatsu R928 photomultiplier tube or a TBX-4-X single-photon-counting detector. Emission and excitation spectra were corrected for source intensity (lamp and grating) and emission spectral response (detector and grating) by standard correction curves. Time-resolved measurements were performed using a (i) Coherent Infinity Nd:YAG-XPO laser (1 ns pulses fwhm) and a Hamamatsu C5680−21 streak camera equipped with a Hamamatsu M5677 low-speed single-sweep unit; (ii) the time-correlated single-photon counting (TCSPC) option on the Fluorolog 3. NanoLEDs (295 or 402 nm; fwhm < 750 ps) with repetition rates between 10 kHz and 1 MHz were used to excite the sample. The excitation sources were mounted directly on the sample chamber at a 90° orientation to a double-grating emission monochromator (2.1 nm/mm dispersion; 1200 grooves/mm) and collected by a TBX-4-X single-photon-counting detector. The photons collected at the detector are correlated by a time-to-amplitude converter to the excitation pulse. Signals were collected using an IBH DataStation Hub photon-counting module, and data analysis was performed using the commercially available *DAS6* software (HORIBA Jobin Yvon IBH). The goodness-of-fit was

(24) Sullivan, B. P.; Salmon, D. J.; Meyer, T. J. *Inorg. Chem.* **1978**, *17*, 3334.
(25) Wilker, W.; Leibfritz, D.; Kerssebaum, R.; Beimel, W. *Magn. Reson. Chem.* **1993**, *31*, 287.
(26) Hurd, R. E. *J. Magn. Reson.* **1990**, *87*, 422.
(27) *Antigona* developed by Dr. Loic Mottier, University of Bologna, Bologna, Italy, 1999.

assessed by minimizing the reduced chi-squared function (χ^2) and by visual inspection of the weighted residuals. Luminescence quantum yields (Φ_{em}) were measured in optically dilute solutions (O.D. < 0.1 at excitation wavelength) and compared to reference emitters by the following equation:[28]

$$\Phi_x = \Phi_r \left[\frac{A_r(\lambda_r)}{A_x(\lambda_x)}\right]\left[\frac{I_r(\lambda_r)}{I_x(\lambda_x)}\right]\left[\frac{n_x^2}{n_r^2}\right]\left[\frac{D_x}{D_r}\right]$$

where A is the absorbance at the excitation wavelength (λ), I is the intensty of the excitation light at the excitation wavelength (λ), n is the refractive index of the solvent, D is the integrated intensity of the luminescence, and Φ is the quantum yield. The subscripts r and x refer to the reference and the sample, respectively. All quantum yields were performed at identical excitation wavelengths for the sample and the reference, canceling the $I(\lambda_r)/I(\lambda_x)$ term in the equation. All ruthenium complexes were measured against Ru(bpy)$_3$Cl$_2$ in air-equilibrated acetonitrile as the reference (Φ = 0.016). All solvents were of spectrometric grade, and all solutions were filtered through a 0.2 μm syringe filter before measurement. Deaerated samples were prepared by the freeze−pump−thaw technique.

Ligand Synthesis. The ligands 2-(*1,H*-tetrazol-5-yl)-pyridine (H**L1**), 2-(*1,H*-tetrazol-5-yl)-pyrazine (H**L2**), and the unreported bis-2,3-(*1H*-tetrazol-5-yl)-pyrazine (H$_2$**L3**) were prepared in acceptable to good yields (80% for H**L1** and H**L2**; 75% for H$_2$**L3**) by following the Demko and Sharpless protocol involving the Zn(II)-assisted 1,3 dipolar cycloaddition of azide anion (N_3^-) onto the appropriate aromatic nitriles.[29] H**L1**: ^{1}H NMR (DMSO-d_6, 400 MHz): 8.76 (d, H$_6$, J = 4.6 Hz), 8.19 (d, H$_3$, J = 7.8 Hz), 8.04 (t, H$_4$, J = 7.8 Hz), 7.59 (t, H$_5$, J = 4.6 Hz) ppm. ^{13}C NMR (DMSO-d_6, 100 MHz): 154.9 (Ct), 150.1 (C$_6$), 143.7 (C$_2$), 138.3 (C$_4$), 126.1 (C$_5$), 122.7 (C$_3$) ppm. H**L2**: ^{1}H NMR (DMSO-d_6, 400 MHz): 9.37 (d, H$_3$, J = 1.2 Hz), 8.85 (m, 2H, H$_5$, H$_6$) ppm. ^{13}C NMR (DMSO-d_6, 100 MHz): 153.5 (Ct), 146.8 (C$_5$), 144.8 (C$_6$), 143.3 (C$_3$), 140.0 (C$_2$) ppm. H$_2$**L3**: ^{1}H NMR (DMSO-d_6, 400 MHz): 9.09 (s, 2H, H$_{5,6}$) ppm. ^{13}C NMR (dmso-d_6, 100 MHz): 153.4 (2 Ct), 146.1 (C$_{5,6}$), 139.8 (C$_{2,3}$) ppm.

The formation of the anions [**L1**]$^-$, [**L2**]$^-$, and [**L3**]$^{2-}$ was achieved by the addition of equimolar amounts (2 equiv in the case of H$_2$**L3**) of triethylamine to a suspension of the neutral 5-substituted tetrazoles in absolute ethanol (5 mL). The resulting pale-yellow solutions were used without any further purification.

Synthesis of the Mononuclear Complexes RuL1 and RuL2. *cis*-[Ru(bpy)$_2$Cl$_2$]·2H$_2$O (0.260 g, 0.50 mmol) was dissolved in dry ethanol (15 mL) in a 100 mL round-bottom flask protected from light. A slight excess (2.2 equiv) of $AgPF_6$ was added, and the mixture was stirred with reflux for 4 h. The reaction mixture was filtered through a Celite pad, and the filtrate was added dropwise to an ethanol (10 mL) solution of the appropriate tetrazolate ligand [**L1**]$^-$ or [**L2**]$^-$ (0.8 mmol). Once the addition was complete, the deep-red solution was stirred at reflux temperature overnight. The mixture was then cooled to r.t., concentrated to about half of the initial volume, added to 10 mL of an aqueous solution containing ca. 0.5 g of NH_4PF_6, and extracted with dichloromethane (3 × 20 mL) until the aqueous phase became colorless. The organic layers were dried over $MgSO_4$, and the solvent was removed in vacuo. The red mixture was redissolved in a minimal quantity of dry acetone, and a copious amount of diethyl ether was added, causing the precipitation of a crude product, which was collected by suction filtration and purified by alumina-filled column chromatography with acetonitrile/toluene mixtures as the eluent. The target mononuclear species were eluted (CH_3CN/toluene 1.2/1, v/v) as the first red band, while elution with pure acetonitrile afforded small quantities of a bis-cationic byproduct identified as [(bpy)$_2$Ru(CH_3CN)$_2$]$^{2+}$. The fractions containing the mononuclear complexes were evaporated to dryness, affording Ru**L1** (0.256 g, 55%) or Ru(**L2**) (0.247 g, 53%) both as deep-red microcrystalline powder. Ru**L1**: ESI-MS: *m/z* 560 [M − PF_6^-]$^+$. ^{1}H NMR (CD_3CN, 400 MHz): 8.47 (t, 2H, J = 8.0 Hz), 8.40 (d, 2H, J = 8.0 Hz), 8.27 (d, *H3*, J = 8.0 Hz), 8.08−7.92 (m, 4H and *H4*), 7.89 (d, 1H, J = 6.0 Hz), 7.85 (d, 1H, J = 6.0 Hz), 7.79 (d, 1H, J = 6.0 Hz), 7.58 (d, 1H, J = 5.6 Hz), 7.56 (d, *H6*, J = 5.6 Hz), 7.44−7.20 (m, 4H and *H5*) ppm. ^{13}C NMR (CD_3CN, 100 MHz) bpys: 158.8, 158.7, 158.3, 158.2 (C-quaternaries), 153.1 (2C), 152.7, 152.6 (N-*ortho* CHs), 138.0, 137.9, 137.85, 137.8 (N-*para* CHs), 128.4, 128.2, 128.1, 127.4, 124.9, 124.8, 124.5, 124.3 (N-*meta* CHs) ppm. Tetrazolate ligand **L1**: 162.9 (*Ct*), 152.5 (*C6*), 151.6 (*C2*), 138.9 (*C4*), 126.6 (*C5*) 123.0 (*C3*) ppm. Anal. Calcd for $C_{26}H_{20}F_6N_9PRu$ (704.59): C, 44.32; H, 2.87; N, 17.90. Found: C, 44.36; H, 2.88; N, 17.88. Ru**L2**: ESI-MS: *m/z* 561 [M − PF_6^-]$^+$. ^{1}H NMR (CD_3CN, 400 MHz): 9.42 (s, *H3*), 8.52−8.40 (m, 4H), 8.39 (d, *H5*, J = 3.3 Hz), 8.08−7.96 (m, 4H), 7.87 (t, 2H, J = 5.5 Hz), 7.78 (d, 1H, J = 5.5 Hz), 7.69 (d, *H6*, J = 3.3 Hz), 7.55 (d, 1H, J = 5.5 Hz), 7.44−7.31 (m, 4H) ppm. ^{13}C NMR (CD_3CN, 100 MHz) bpys: 158.6, 158.3, 158.1, 158.0 (C-quaternaries), 153.2, 153.0 152.8 (2C) (N-*ortho* CHs), 138.5, 138.4, 138.32, 128.29 (N-*para* CHs), 128.7, 128.34, 128.26, 127.6, 125.1, 125.0, 124.6, 124.4 (N-*meta* CHs); tetrazolate ligand **L2**, 161.2 (*Ct*), 147.5 (*C2*), 147.3 (*C5*), 146.8 (*C6*), 143.6 (*C3*) ppm. Suitable crystals for X-ray diffraction experiments were obtained by the slow diffusion of diethyl ether into a dichloromethane solution of the complex Ru**L2**, which crystallized as [Ru**L2**][PF_6]·0.5Et$_2$O·0.5H$_2$O. Anal. Calcd for $C_{27}H_{25}F_6N_{10}OPRu$ (751.61): C, 43.14; H, 3.33; N, 18.64. Found: C, 43.12; H, 3.33; N, 18.66.

Synthesis of the Dinuclear Complex Ru(L3)Ru. The target bimetallic compound Ru(**L3**)Ru was prepared by following a procedure analogous to that reported above for the mononuclear species. The only difference was represented by the fact that the reactive species obtained from the Ag(I)-mediated chloride extraction of *cis*-[Ru(bpy)$_2$Cl$_2$]·2H$_2$O (0.260 g, 0.50 mmol) was combined with an ethanol solution (5 mL) containing 0.5 equiv (calculated with respect to the starting *cis*-[Ru(bpy)$_2$Cl$_2$]·2H$_2$O) of the tetrazolate ligand $\mathbf{L3}^{2-}$. Then, the deep-red mixture was stirred at reflux temperature for 15 h, and the subsequent anion exchange procedure with aqueous NH_4PF_6 afforded a crude dark-red product, which was purified by alumina-filled column chromatography. The dinuclear complex Ru(**L3**)Ru (0.107 g, 40%) was obtained as the final red-purple fraction (acetonitrile/toluene/methanol 70/30/0.5 (v/v)) following small amounts of a presumably trinuclear (M^{4+} = 364 *m/z*) byproduct. Ru(**L3**)Ru: ESI-MS: *m/z* 521 [M − 2PF_6^-]$^{2+}$. ^{1}H NMR (CD_3CN, 600 MHz): **L3** 7.30 (s, 2H, *H5* and *H6*) ppm. ^{13}C NMR (CD_3CN, 100 MHz) bpys: 158.6, 158.3, 158.1, 158.0 (C-quaternaries), 153.2, 153.0 152.8 (2C) (N-*ortho* CHs), 138.5, 138.4, 138.32, 128.29 (N-*para* CHs), 128.7, 128.34, 128.26, 127.6, 125.1, 125.0, 124.6, 124.4 (N-*meta* CHs); tetrazolate ligand **L3**, 161.5 (*Ct*), 146.6 (*C5*, *C6*), 146.2 (*C2*, *C3*) ppm. Anal. Calcd for $C_{46}H_{34}N_{18}Ru_2P_2F_{12}$ (1332.06): C, 41.44; H, 2.57; N, 18.92. Found: C, 41.52; H, 2.45; N, 19.15.

General Procedure for the Methylation of RuL1 and RuL2. A portion of 0.15 mmol of the starting mononuclear complex Ru**L1** or Ru**L2** was dissolved in dichloromethane (10 mL) under an argon atmosphere with stirring, and the resulting deep-red solution was

(28) Eaton, D. F. *Pure Appl. Chem.* **1988**, *60*, 1107.
(29) Demko, Z. P.; Sharpless, K. B. *J. Org. Chem.* **2001**, *66*, 7945.

Table 5. Crystal Data and Experimental Details for [Ru**L2**][PF_6]·0.5Et_2O·0.5H_2O, [Ru**L1**Me][PF_6]$_2$·CH_3CN, and [Ru**L2**Me][PF_6]$_2$·CH_3CN

complex	[Ru**L2**][PF_6]·0.5Et_2O·0.5H_2O	[Ru**L1**Me][PF_6]$_2$·CH_3CN	[Ru**L2**Me][PF_6]$_2$·CH_3CN
formula	$C_{27}H_{25}F_6N_{10}OPRu$	$C_{29}H_{26}F_{12}N_{10}P_2Ru$	$C_{28}H_{25}F_{12}N_{11}P_2Ru$
fw	751.61	905.61	906.60
T, K	293(2)	298(2)	293(2)
λ, Å	0.71073	0.71073	0.71073
cryst syst	monoclinic	triclinic	triclinic
space group	$C2/c$	$P\bar{1}$	$P\bar{1}$
a, Å	29.426(6)	9.7010(8)	10.6288(7)
b, Å	13.159(3)	13.6667(11)	12.8757(8)
c, Å	16.647(3)	14.0902(11)	14.5384(9)
α, deg	90	81.4510(10)	71.8820(10)
β, deg	111.10(3)	71.4870(10)	74.5710(10)
γ, deg	90	89.5220(10)	71.7250(10)
cell volume, Å^3	6014(2)	1750.2(2)	1764.02(19)
Z	8	2	2
D_c, g cm^{-3}	1.660	1.718	1.707
μ, mm^{-1}	0.654	0.643	0.638
F(000)	3024	904	904
crystal size, mm	0.23 × 0.19 × 0.12	0.25 × 0.20 × 0.15	0.21 × 0.18 × 0.13
θ limits, deg	1.48−25.02	1.51−25.00	1.50−25.03
reflns collected	26 064	16 659	16 981
independent reflns	5314 [R_{int} = 0.0655]	6137 [R_{int} = 0.0196]	6223 [R_{int} = 0.0198]
data/restraints/parameters	5314/3/416	6137/54/516	6223/0/498
GOF on F^2	1.031	1.064	1.059
R_1 ($I > 2\sigma(I)$)	0.0506	0.0426	0.04044
R_2 (all data)	0.1518	0.1234	0.1169
largest diff peak and hole, e·Å^{-3}	0.971/−0.632	1.030/−0.534	1.009/−0.718

cooled to −50 °C. Methyl triflate (1 mL, 0.150 M in dichloromethane, 0.150 mmol) was successively added dropwise to the vigorously stirred solution. After 30 min at −50 °C, the red mixture was allowed to warm to r.t. and stirred for an additional 6 h. Evaporation of the solvent afforded a red oily residue which was dissolved into a minimal amount of acetonitrile and added to 10 mL of an aqueous solution containing ca. 0.5 g of NH_4PF_6. The resulting mixture was extracted with dichloromethane (3 × 20 mL) until the aqueous phase became colorless. The organic layers were dried over $MgSO_4$, and the solvent was removed in vacuo, affording a crude product which was purified by alumina-filled column chromatography with acetonitrile/toluene mixtures as the eluent. The bis-cationic methylated species Ru**L1**Me (0.105 g, 81%) and Ru**L2**Me (0.095 g, 73%) were recovered as a red band after a first fraction, represented by the starting complexes. However, small amounts of Ru**L1** and Ru**L2** were found to contaminate the batches of the methylated derivatives. Repeated re-crystallizations from acetone/diethyl ether (1/2, v/v) mixtures allowed us to minimize and, in some cases, to almost eliminate their presence. Ru**L1**Me: ESI-MS: m/z 287 [M − 2PF_6^-]$^{2+}$. ^{1}H NMR (CD_3CN, 400 MHz): 8.54−8.44 (m, 4H), 8.39 (d, *H3*, J = 8.0 Hz), 8.13−8.06 (m, 3H and *H4*), 8.04−7.98 (m, 2H), 7.84−7.80 (m, 2H), 7.77 (d, *H6*, J = 5.6 Hz), 7.71 (d, 1H, J = 5.6 Hz), 7.51−7.43 (m, 4H), 7.38−7.34 (m, *H5*), 4.39 (s, 3H, *Me*) ppm. ^{13}C NMR (CD_3CN, 100 MHz) bpys: 158.7, 158.4, 158.0, 157.8 (C-quaternaries), 153.4, 153.3, 153.2, 153.1 (N-*ortho* CHs), 139.1, 139.03, 139.00, 138.97 (N-*para* CHs), 128.8, 128.7, 128.6, 128.0, 125.4, 125.36, 125.3, 125.0 (N-*meta* CHs); tetrazolate ligand **L1**Me, 166.1 (*Ct*), 153.7 (*C6*), 147.2 (*C2*), 139.9 (*C4*), 129.7 (*C5*) 124.6 (*C3*), 42.9 (*Me*) ppm. Crystals suitable for X-ray analysis were obtained by the slow diffusion of diethyl ether into an acetonitrile solution of the complex, which crystallized as [Ru**L1**Me][PF_6]$_2$·CH_3CN. Anal. Calcd for $C_{29}H_{26}F_{12}N_{10}P_2Ru$ (905.61): C, 38.46; H, 2.90; N, 15.47. Found: C, 38.47; H, 2.89; N, 15.50. Ru**L2**Me: ESI-MS: m/z 288 [M − 2PF_6^-]$^{2+}$. ^{1}H NMR (CD_3CN, 400 MHz): 9.50 (d, *H3*, J = 1.2 Hz), 8.59 (d, *H5*, J = 3.2 Hz), 8.52−8.45 (m, 4H), 8.14−8.02 (m, 4H), 7.89 (d, 1H, J = 6.4 Hz), 7.84 (d, 1H, J = 5.6 Hz) 7.80 (d of d, *H6*, J_1 = 3.2 Hz, J_2 = 1.2 Hz), 7.75 (d, 1H, J = 5.6 Hz), 7.73−7.70 (m, 2H), 7.48−7.36 (m, 4H), 4.41 (s, 3H, *Me*) ppm. ^{13}C NMR (CD_3CN, 100 MHz) bpys: 158.3, 158.2, 157.7, 157.67 (C-quaternaries), 153.8, 153.5, 153.2, 153.1 (N-*ortho* CHs), 139.56, 139.54, 139.5, 139.4 (N-*para* CHs), 128.9 (2C), 128.7, 128.1, 125.5, 125.4, 125.1, 124.8 (N-*meta* CHs); tetrazolate ligand **L2**Me, 164.7 (*Ct*), 149.9 (*C5*), 148.5 (*C6*), 145.3 (*C3*), 143.5 (*C2*), 43.1 (*Me*) ppm. Crystals suitable for X-ray analysis were obtained by the slow diffusion of diethyl ether into an acetonitrile solution of the complex, which crystallized as [Ru**L2**Me][PF_6]$_2$·CH_3CN. Anal. Calcd for $C_{28}H_{25}F_{12}N_{11}P_2Ru$ (906.60): C, 37.09; H, 2.78; N, 17.00. Found: C, 37.07; H, 2.79; N, 17.05.

X-ray Crystallography. Crystal data and collection details are reported in Table 5. The diffraction experiments were carried out on a Bruker APEX II diffractometer (for [Ru**L2**Me][PF_6]$_2$·CH_3-CN and [Ru**L1**Me][PF_6]$_2$·CH_3CN) and on a Bruker SMART 2000 diffractometer (for [Ru**L2**][PF_6]·0.5Et_2O·0.5H_2O), equipped with a CCD detector and using Mo Kα radiation. Data were corrected for Lorentz polarization and absorption effects (empirical absorption correction program *SADABS*).[30] Structures were solved by direct methods and refined by full-matrix least-squares procedures based on all data using F^2.[31] H atoms were placed in calculated positions, except the independent hydrogen in the water molecule, H(10), in [Ru**L2**][PF_6]·0.5Et_2O·0.5H_2O, which was located in the Fourier map and refined with the O(2)−H(10) distance restrained to 0.84 Å. H atoms were treated isotropically using the 1.2 fold U_{iso} value of the parent atom, except methyl and water protons, which were assigned the 1.5 fold U_{iso} value of the parent C atom and O atom, respectively. All non-hydrogen atoms were refined with anisotropic displacement parameters, unless otherwise stated.

Acknowledgment. The authors wish to thank the Italian Ministero dell'Istruzione, Università e Ricerca (M.I.U.R.) (PRIN 2004035330 and 2004030719) for financial support. The Faculty of Industrial Chemistry of the University of

(30) Sheldrick, G. M. *SADABS*; University of Göttingen: Göttingen, Germany, 1996.
(31) Sheldrick, G. M. *SHELX97, Program for the Refinement of Crystal Structure*; University of Göttingen: Göttingen, Germany, 1997.

Bologna is gratefully acknowledged for a post-graduate research grant (to E.O.). The authors also wish to thank one of the reviewers for useful suggestions.

Supporting Information Available: ^{1}H and ^{13}C NMR spectra of all complexes, cyclic voltammetries of Ru**L2** and Ru**L2**Me in PDF format; X-ray crystallographic files in CIF format for the crystal structure determinations of complexes Ru**L2**, Ru**L2**Me, and Ru**L1**Me. This material is available free of charge via the Internet at http://pubs.acs.org.

IC7011556